Reversible control of ionic conductivity and viscoelasticity of organometallic ionic liquids by application of light and heat

Sumitani, Ryo
Yoshikawa, Hirofumi
Mochida, Tomoyuki

(Citation)
Chemical Communications,56(46):6189-6192

(Issue Date)
2020-06-11

(Resource Type)
journal article

(Version)
Accepted Manuscript

(URL)
https://hdl.handle.net/20.500.14094/90007203

Reversible Control of Ionic Conductivity and Viscoelasticity of Organometallic Ionic Liquids by Application of Light and Heat

Ryo Sumitani, [a] Hirofumi Yoshikawa [b] and Tomoyuki Mochida *[ac]

Received 00th January 20xx,
Accepted 00th January 20xx

DOI: 10.1039/x0xx00000x

Ru-containing ionic liquids $[Ru(C_5H_5)\{C_6H_3(OC_6H_{12}CN)_3\}][N(SO_2F)_2]$ (1) and $[Ru(C_5H_5)\{C_6H_5(OC_3H_6CN)\}][N(SO_2F)_2]$ (2), having different numbers of substituents, were reversibly converted to coordination polymer solids and oligomeric liquids, respectively, by UV photoirradiation and heating. This feature enabled the control of their ionic conductivities and viscoelastic properties.

Ionically conducting materials, including superionic conducting solids,[1a] polymers,[1b] and ionic liquids,[1c] have been used for a wide range of electronic applications such as capacitors and chemical sensors. The addition of photocontrollability to their ionic conductivity should greatly enhance their utility. Currently, however, there are very few examples of photocontrollable ionic conductors. A photoswitchable ionically conductive coordination polymer with a photoisomerizable ligand was recently reported.[2] Polymers containing photochromic moieties can reversibly change their ionic conductivity upon photoirradiation, albeit with small ionic conductivity change.[3,4] Ionic liquids containing azobenzene units exhibit reversible ionic conductivity changes owing to solid-liquid transformations based on photoisomerization.[5] Such a photoisomerization mechanism is a useful strategy for controlling ionic conductivity. However, the photochemical immobilization of ions should enable a more straightforward and flexible control of ionic conductivity, if the process is thermally or photochemically reversible.

The purpose of this study is to demonstrate the photochemical control of ionic conductivity based on a mechanism of bond transformation in ionic liquids. Ionic liquids are useful for electronic devices owing to their high ionic conductivity and negligible vapor pressure.[6] As part of our continuing studies on functional ionic liquids containing organometallic cations,[7] we previously reported ruthenium-containing organometallic ionic liquid **1** ($[Ru(C_5H_5)\{C_6H_3(OC_6H_{12}CN)_3\}][N(SO_2F)_2]$, Fig. 1a), which reversibly transforms to an amorphous coordination polymer by the application of ultraviolet (UV) light and heat (Fig. 2).[8] Photoirradiation of **1** causes dissociation of the arene ligand, followed by the coordination of the three cyano groups to the Ru ion, which leads to gradual solidification owing to the formation of a three-dimensionally cross-linked structure. Furthermore, the reaction can be reversed by heating. Since this transformation involves reversible fixation of the constituent ions, we hypothesized that the mechanism could be used for the control of ionic conductivity.

This paper reports the reversible control of the viscoelasticity and ionic conductivity of Ru-containing ionic liquids **1** and **2** ($[Ru(C_5H_5)\{C_6H_5(OC_3H_6CN)\}][N(SO_2F)_2]$) (Fig. 1) by the application of light and heat. These ionic liquids, having different numbers of substituents, exhibit glass transitions at −53 °C[8] and −60 °C,[9] respectively. The photoreactivity of **2** was investigated for the first time in this study. In addition, the photoreaction mechanism for **1** was investigated by X-ray absorption fine structure (XAFS) analysis.

As reported previously, pale yellow liquid **1** changes into a yellow elastomer upon UV photoirradiation in approximately 4 to 6 h.[8] The time course of the reaction is shown in Fig. 3. The

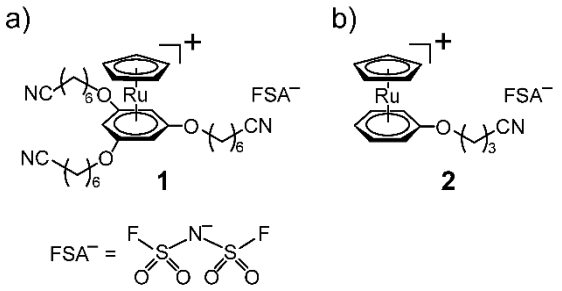

Fig. 1 Structural formulae of ionic liquids (a) **1** and (b) **2**.

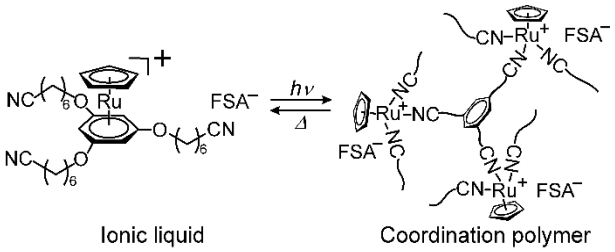

Fig. 2 Reversible transformation between ionic liquid **1** and amorphous coordination polymer by application of light and heat.

[a] Department of Chemistry, Graduate School of Science, Kobe University
1-1 Rokkodai, Nada, Kobe, Hyogo 657-8501, Japan.
E-mail: tmochida@platinum.kobe-u.ac.jp
[b] School of Science & Technology, Kwansei Gakuin University
2-1 Gakuen, Sanda, Hyogo 669-1337, Japan.
[c] Center for Membrane Technology, Kobe University
1-1 Rokkodai, Nada, Kobe, Hyogo 657-8501, Japan

†Electronic Supplementary Information (ESI) available: EXAFS spectra, XANES spectra, NMR spectra, and viscosity data. See DOI: 10.1039/x0xx00000x

reaction rate, i.e., the molar ratio of the photoreacted species, becomes saturated at approximately 80% because unreacted complexes are trapped inside the solid.[8] We performed Ru *K*-edge XAFS measurements of **1** before and after the photoreaction (Fig. S1, ESI†). Analysis of the spectra revealed that, after photoirradiation, the coordination bond lengths are shortened owing to Ru–N bond formation and the Ru oxidation state is unchanged, which support the reaction mechanism shown in Fig. 2.

In contrast, **2** exhibits no solidification upon UV photoirradiation; this liquid changes from a pale yellow liquid to a highly viscous yellow liquid in 15 min, when the reaction rate is saturated at approximately 93% (Fig. 3). The reaction speed is considerably faster than that of **1** partly because of its low viscosity. Since three cyano groups are coordinated to the Ru ion, this photoreaction produces a complex in which an arene ligand and two cations are coordinated to the dissociated Ru complex (Fig. 4). The observed ratio of the photodissociated cation in the product is nearly one-third (28%), which is consistent with the reaction mechanism. The ^{1}H, ^{13}C NMR (Fig. S2 and S3, ESI†), and ESI-MS spectra (*m/z*: calcd 328.0275; found 328.0280) in dichloromethane are consistent with the structure, though complexes with different combinations of ligands may also be present in the product. Heating the photoproduct at 120 °C quantitatively recovers **2** within 10 min, similarly to the case of **1**. The changes in the ^{1}H NMR and UV-Vis spectra associated with this reversible transformation are shown in Fig. 5.

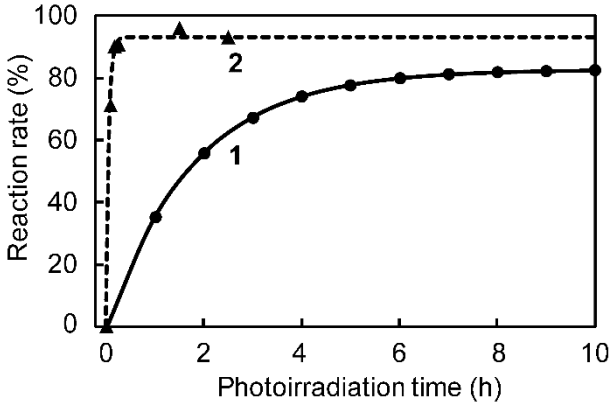

Fig. 3 Time course of the reaction, where the reaction rate is given by the molar ratio of the photoreacted species in the products generated by photoirradiation of **1** (—) and **2** (----) as determined from the UV-Vis spectral absorbance at 365 nm and ^{1}H NMR spectra.

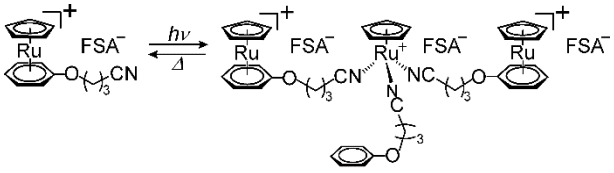

Fig. 4 Reversible transformation between ionic liquid **2** and its oligomer by application of light and heat.

Next, the viscoelastic changes of **1** and **2** upon photoirradiation were investigated. The viscosity of **1** is 2.6 Pa·s (shear rate, 1 s^{-1}; 25 °C). The frequency dependence of the storage modulus (*G*′) and loss modulus (*G*″) of **1** is shown in Fig. 6a. The modulus values at low frequency are approximately 10^{1} Pa before photoirradiation, but increase by four orders of magnitude after 8 h photoirradiation, when the reaction rate is 55%. The photoreaction speed was slower than that shown in Fig. 3 because of sample thickness. Before photoirradiation, *G*″ exceeds *G*′ over the entire measurement range (1–100 rad s^{-1}), indicating viscous behavior (tan $\delta = G''/G' > 1$). However, after 4 and 8 h photoirradiation, *G*′ exceeds *G*″ (tan $\delta < 1$) in the range above 6 and 4 rad s^{-1}, respectively, thereby indicating the change to an elastomer. The complex viscosity increases greatly from 4.0 Pa·s to 1.2 × 10^{5} Pa·s (at 2.5 rad s^{-1}) after 8 h photoirradiation (Fig. 6b). Longer photoirradiation may increase the reaction rate and viscosity even further.

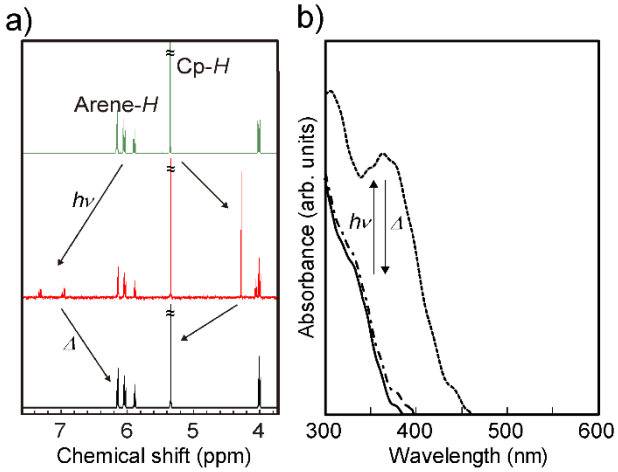

Fig. 5 (a) ^{1}H NMR spectra (400 MHz, CD_3CN) and (b) UV-Vis spectra of **2** before (—) and after photoirradiation for 2.5 h (----), and after subsequently heating at 120 °C for 10 min (-·-·-). In the ^{1}H NMR spectra, the photodissociated cation is observed as $[Ru(Cp)(CD_3CN)_3]^{+}$ owing to ligand exchange by the solvent.

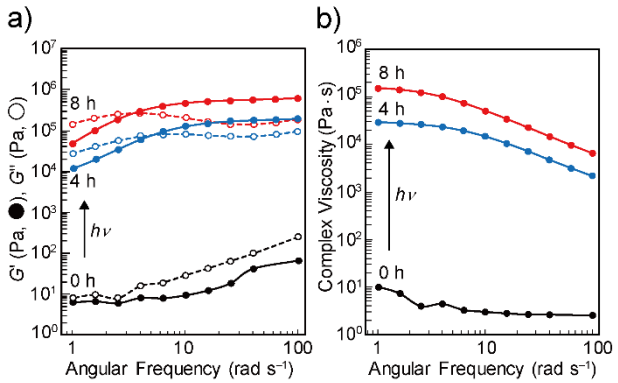

Fig. 6 (a) Frequency dependence of the storage modulus *G*′ (●) and loss modulus *G*″ (○) of **1** before and after 4 and 8 h UV photoirradiation. (b) Frequency dependence of the complex viscosity of **1** before and after photoirradiation (25 °C, strain 1%).

Table 1 Ionic conductivity (25 °C), viscosity, Walden product, and glass transition temperature of ionic liquids **1** and **2** before and after UV photoirradiation.

Compound	Ionic conductivity (mS cm^{-1})		Viscosity (mPa s)		Walden product	T_g (°C)[a]
	Before	After	Before	After	(mPa s mS cm^{-1})[a]	
1	3.1×10^{-2}	4.8×10^{-4} [b]	2.60×10^{3}	1.2×10^{8} [d]	81	−53 [e]
2	4.0×10^{-1}	3.7×10^{-2} [c]	9.2×10^{2}	5.2×10^{3} [d]	370	−60 [f]

[a] Before photoirradiation. [b] After 2 h photoirradiation. [c] After 10 min photoirradiation. [d] After 8 h photoirradiation. [e] Ref. 8. [f] Ref. 9.

In contrast, the viscosity of **2** at 25 °C is 0.9 Pa·s. This liquid is less viscous than **1** (2.6 Pa·s at 1 s^{-1}) owing to the lower number of substituents, which is consistent with the lower glass transition temperature of **2** than **1**. The viscosity after photoirradiation for 8h (reaction rate 84%) is 5.2 Pa·s, which is an increase of approximately 6 times (Fig. S4, ESI†). The increase is much smaller than that observed in **1** because the photoproduct is also a liquid in this case. Liquid **2** is a Newtonian fluid both before and after the photoreaction.

Based on these results, the control of the ionic conductivities of **1** and **2** by the application of light and heat was investigated. Table 1 summarizes the ionic conductivity, viscosity, and Walden product values of **1** and **2** at 25 °C. Their ionic conductivities are 3.1×10^{-2} and 4.0×10^{-1} mS cm^{-1}, respectively, and the higher ionic conductivity of the latter is consistent with its lower viscosity. Both the cation and anion are responsible for the ionic conductivity, and the Walden products, i.e., the product of ionic conductivity and solution viscosity, are comparable to those of other ionic liquids.[10] The smaller Walden product of **1** than **2** is ascribed to its larger cation volume.

Photoirradiation of these liquids results in the decrease of ionic conductivity owing to bond formation between the cations, which reduces their mobility. Irradiation of **1** reduces its ionic conductivity by two orders of magnitude in 2 h (Fig. 7a). Subsequent heating of the sample at 120 °C for 10 min recovers the conductivity through the reverse reaction, as expected. Changes in ionic conductivity caused by alternate hourly cycles of photoirradiation and heating are shown in Fig. 7b (dashed line). The changes are smaller for a 10-min cycle (Fig. 7b, solid line). Photoirradiation of **2** decreases its ionic conductivity by one order of magnitude in 15 min (Fig. 8a), and heating at 120 °C recovers the initial value. Thus, its photoresponse is considerably faster than that of **1**. The change in ionic conductivity is larger than that in 1 for the 10-min cycle (Fig. 8b).

There are various organic polymers that exhibit viscoelastic changes or reversible bond formation by the application of light and heat,[11] but few exhibit changes in ionic conductivity.[4] There are several ionic[5,12] and molecular[13] materials that display solid-liquid changes by the application of light and heat. Among them, azobenzene-containing ionic liquids exhibit on-off control of the ionic conductivity based on the phase change.[5] The current system, however, exhibits continuous structural changes from an ionic liquid to a networked or oligomeric structure, thereby enabling flexible control of the ionic conductivity. The

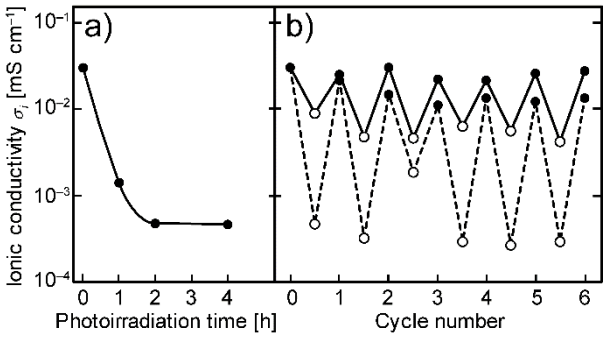

Fig. 7 (a) Time course of ionic conductivity (25 °C) of **1** upon UV irradiation. (b) Ionic conductivity changes of **1** for alternating hourly (---) or 10 min (—) cycles of UV photoirradiation (open circles) and 120 °C heating (filled circles).

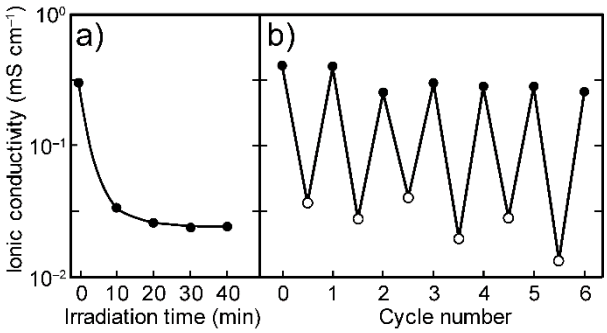

Fig. 8 (a) Time course of ionic conductivity of **2** upon UV irradiation (25 °C). (b) Ionic conductivity changes of **2** for alternating 10 min (—) cycles of UV photoirradiation (open circles) and heating at 120 °C (filled circles).

reactivities of ruthenium complexes is versatile to fabricate such stimuli-responsive materials. Several ruthenium-containing polymers that exhibit intriguing redox- and photo-responsivity are reported recently.[14]

In summary, this study has shown that reversible control of the ionic conductivity and viscoelasticity of Ru-containing ionic liquids is possible by the application of light and heat. The physical property changes are based on the reversible formation of intermolecular bonds. It is noteworthy that the numbers of substituents caused striking changes in the photoproducts, i.e., either a three-dimensional coordination polymer solid or an oligomeric liquid. Accordingly, the viscoelasticity changes, reaction rates, and physical properties of the materials were tunable by their substituents. Their ionic

liquid characteristics, such as nonvolatility, are advantageous for applications such as photocontrollable capacitors, sensors, and other electronic devices. Moreover, the strategy of using reversible bond formation by external stimuli, as demonstrated here, can be extended to the development of other functions such as photochemical gelation and lubricity control.

This work was financially supported by The Canon Foundation and a KAKENHI grant (Nos. 18H04516 and 18H04528) from the Japan Society for the Promotion of Science (JSPS).

Conflicts of interest

There are no conflicts to declare.

Notes and references

1 (*a*) T. Takahashi, *High Conductivity Solid Ionic Conductors: Recent Trends and Applications*, World Scientific, Singapore, 1989; (*b*) V. Di Noto, S. Lavina, G. A. Giffin, E. Negro and B. Scrosati, *Electrochim. Acta*, 2011, **57**, 4–13; c) M. Armand, F. Endres, D. R. MacFarlane, H. Ohno and B. Scrosati, *Nat. Mater.*, 2009, **8**, 621–629.

2 S. Ohkoshi, K. Nakagawa, K. Imoto, H. Tokoro, Y. Shibata, K. Okamoto, Y. Miyamoto, M. Komine, M. Yoshikiyo and A. Namai, *Nat. Chem.*, 2020, **12**, 338–344.

3 (*a*) H. Nie, N. S. Schauser, N. D. Dolinski, J. Hu, C. J. Hawker, R. A. Segalman and J. Read de Alaniz, *Angew. Chem. Int. Ed.*, 2020, **59**, 5123–5128; (*b*) H. Mochizuki, Y. Nabeshima, T. Kitsunai, A. Kanazawa, T. Shiono, T. Ikeda, T. Hiyama, T. Maruyama, T. Yamamoto and N. Koide, *J. Mater. Chem.*, 1999, **9**, 2215–2219; (*c*) H. Tokuhisa, M. Yokoyama and K. Kimura, *J. Mater. Chem.*, 1998, **8**, 889–891.

4 H. Wang, C. N. Zhu, H. Zeng, X. Ji, T. Xie, X. Yan, Z. L. Wu and F. Huang, *Adv. Mater.*, 2019, **31**, 1807328.

5 K. Ishiba, M. Morikawa, C. Chikara, T. Yamada, K. Iwase, M. Kawakita and N. Kimizuka, *Angew. Chem. Int. Ed.*, 2015, **54**, 1532–1536.

6 M. Kar, K. Matuszek and D. R. MacFarlane, *Ionic Liquids in Kirk–Othmer Encyclopedia of Chemical Technology*, Wiley, Hoboken, 2019.

7 (*a*) T. Inagaki, T. Mochida, M. Takahashi, C. Kanadani, T. Saito and D. Kuwahara, *Chem. Eur. J.*, 2012, **18**, 6795–6804; (*b*) T. Ueda, T. Tominaga, T. Mochida, K. Takahashi and S. Kimura, *Chem. Eur. J.*, 2018, **24**, 9490–9493; (*c*) T. Tominaga and T. Mochida, *Chem. Eur. J.*, 2018, **24**, 6239–6247.

8 Y. Funasako, S. Mori and T. Mochida, *Chem. Commun.*, 2016, **52**, 6277–6279.

9 A. Komurasaki, Y. Funasako and T. Mochida, *Dalton Trans.*, 2015, **44**, 7595–7605.

10 (*a*) W. Xu, E. I. Cooper and C. A. Angell, *J. Phys. Chem. B*, 2003, **107**, 6170–6178; (*b*) D. R. MacFarlane, M. Forsyth, E. I. Izgorodina, A. P. Abbott, G. Annat and K. Fraser, *Phys. Chem. Chem. Phys.*, 2009, **11**, 4962–4967.

11 (*a*) I. Teasdale, S. Theis, A. Iturmendi, M. Strobel, S. Hild, J. Jacak, P. Mayrhofer and U. Monkowius, *Chem. Eur. J.*, 2019, **25**, 9851–9855; (*b*) R. J. Wojtecki, M. A. Meador and S. J. Rowan, *Nat. Mater.*, 2011, **10**, 14–27; (*c*) J. Kida, D. Aoki and H. Otsuka, *ACS Macro Lett.*, 2019, **8**, 1–6; (*d*) J. V. Accardo and J. A. Kalow, *Chem. Sci.*, 2018, **9**, 5987–5993; (*e*) G. Pouliquen, C. Amiel and C. Tribet, *J. Phys. Chem. B*, 2007, **111**, 5587–5595; (*f*) I. Tomatsu, A. Hashidzume and A. Harada, *Macromolecules*, 2005, **38**, 5223–5227.

12 (*a*) S. Hisamitsu, N. Yanai, S. Fujikawa and N. Kimizuka, *Chem. Lett.*, 2015, **44**, 908–910; (*b*) H. Tamura, Y. Shinohara and T. Arai, *Chem. Lett.*, 2011, **40**, 129–131.

13 (*a*) W. Xu, S. Sun and S. Wu, *Angew. Chem., Int. Ed.*, 2019, **58**, 9712–9740; (*b*) T. Yamamoto, Y. Norikane and H. Akiyama, *Polym. J.*, 2018, **50**, 551–562.

14 H. Zhou, M. Chen, Y. Liu and S. Wu, *Macromol. Rapid Commun.*, 2018, **39**, 1800372.

Graphical abstract

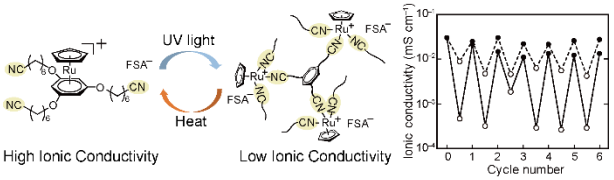

Ruthenium-containing ionic liquids were reversibly converted to amorphous coordination polymers or oligomeric liquids by the alternate application of ultraviolet light or heat, thus enabling reversible control of their ionic conductivity and viscoelasticity.

Supporting Information

Reversible Control of Ionic Conductivity and Viscoelasticity of Organometallic Ionic Liquids by Application of Light and Heat

Ryo Sumitani,[a] Hirofumi Yoshikawa,[b] and Tomoyuki Mochida*[a,c]

[a]*Department of Chemistry, Graduate School of Science, Kobe University, 1-1 Rokkodai, Nada, Kobe, Hyogo 657-8501, Japan, E-mail: tmochida@platinum.kobe-u.ac.jp*

[b]*School of Science & Technology, Kwansei Gakuin University, 2-1 Gakuen, Sanda, Hyogo 669-1337, Japan*

[c]*Center for Membrane Technology, Kobe University, 1-1 Rokkodai, Nada, Kobe, Hyogo 657-8501, Japan*

Table of Content

Experimental details

XAFS Analysis

Fig. S1 Ru K-edge (a) EXAFS and (b) XANES spectra of **1** before and after photoirradiation.

Table S1 Parameters derived from the simulation of the EXAFS spectra of **1** before and after photoirradiation

Fig. S2 ^{13}C NMR spectra of (a) **2** and (b) its photoproduct in CD_2Cl_2.

Fig. S3 ^{1}H NMR spectra of (a) **2** and (b) its photoproduct in CD_2Cl_2.

Fig. S4 Viscosity of ionic liquid **2** before and after photoirradiation (8 h).

Experimental details

General. Ionic liquids **1** and **2** were synthesized according to the procedure in the literature.[S1,S2] ^{1}H and ^{13}C NMR spectra were recorded using Bruker Avance 400 instruments (400 MHz). Dynamic viscoelasticity was measured using a TA Instruments DHR-2 rheometer equipped with a ϕ8 mm parallel plate. The frequency dependence of the dynamic viscoelasticity (1–100 rad s^{-1}) was measured at 25 °C under an application of 1% strain. Ionic conductivity was measured using a Solartron 1260 impedance analyzer. Gold interdigitated electrodes with gap dimensions of 200 μm were used; the cell constant was determined by measuring the conductivity of 0.01 M KCl aqueous solution at 25 °C. Electrospray ionization–mass spectrometry (ESI-MS) was performed using a Thermo Fisher Scientific LTQ-Orbitrap Discovery instrument. An LED light source (Hamamatsu Photonics LC-L1V3, 0.6 W cm^{-2}) was used for UV photoirradiation. Photoirradiation experiments were conducted on samples sandwiched between two quartz plates. The samples used for the viscoelasticity measurements were thicker than those used in other experiments; hence, the photoreaction speed was considerably slower.

XAFS measurements. Ex situ Ru *K*-edge X-ray absorption fine structure (XAFS) measurements were carried out in transmission mode at room temperature, using the BL14B1 beam lines at SPring-8 (8.0 GeV, 100 mA). X-rays from a bending magnet were monochromatized by a Si(111) double-crystal monochromator. The intensities of the incident (I_0) and transmitted (I_t) X-rays were detected by ion chambers. RuO_2 and $RuCl_3$ diluted with boron nitride were used as standard materials. The X-ray absorption near edge structure (XANES) spectra were obtained by pre-edge background subtraction and subsequent normalization using Athena software. Extended X-ray absorption fine structure (EXAFS) spectra were analysed by standard procedures using the Ifeffit (Artemis) program. The extracted

k^3-weighted Ru K-edge EXAFS oscillations (3–11 $Å^{-1}$) were Fourier-transformed into R-space, in which curve-fitting analysis was performed.

XAFS Analysis

The normalised Ru *K*-edge XANES spectra in **Fig. S1a** exhibit no obvious variation before and after photoirradiation, indicating that the valence of Ru was maintained at its initial oxidation state. **Fig. S1b** shows the k^3-weighted Fourier-transform (FT) Ru *K*-edge EXAFS spectra recorded before and after photoirradiation. Curve fitting of the EXAFS spectra was performed using parameters for the backscattering amplitudes and phase shifts of the appropriate Ru−C and Ru−N shells, which were obtained from the crystal structure data of related compounds. The peak at 1.73 Å in **1** was analyzed using the bond lengths in $[Ru(Cp)(C_6H_5Bu)]^+$,[S2] whereas the peak at 1.69 Å of the sample after photoirradiation was analyzed using the bond lengths in $[Ru(Cp)(MeCN)_3]^+$.[S3] The interatomic distances and coordination numbers were obtained as fitting variables for all cases (**Table 1**), while the Debye−Waller factors and energy shift (Δ*E*) values were fixed. The simulated curves explain the curvatures of the experimental spectra fairly well, supporting the formation of Ru−N bonds upon photoirradiation.

References

S1. Y. Funasako, S. Mori and T. Mochida, *Chem. Commun.*, **2016**, *52*, 6277-6279.

S2. A. Komurasaki, Y. Funasako and T. Mochida, *Dalton Trans.*, **2015**, *44*, 7595-7605.

S3. A. Trujillo, F. Justaud, L. Toupet, O. Cador, D. Carrillo, C. Manzur and J.-R. Hamon, *New J. Chem.*, **2011**, *35*, 2027-2036.

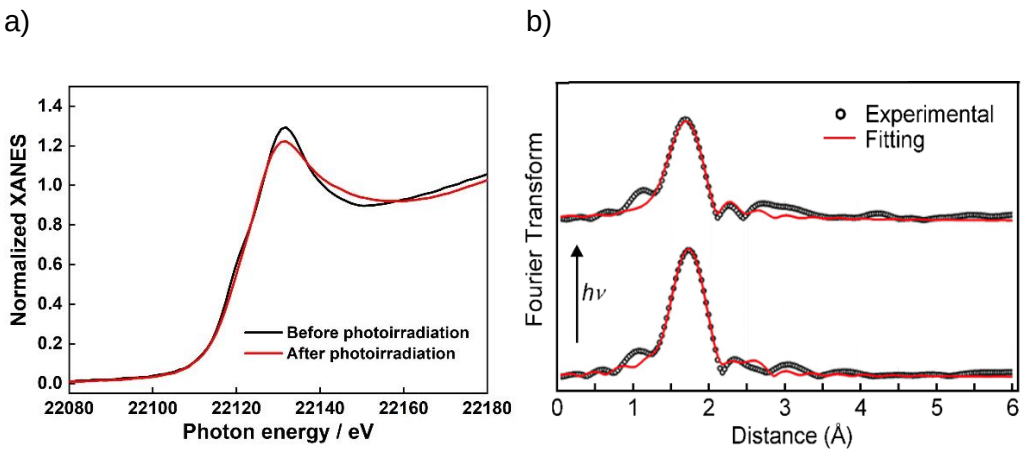

Fig. S1 Ru K-edge (a) XANES spectra and (b) EXAFS spectra of **1** before and after photoirradiation. Fitting curves are also shown in (b).

Table S1 Parameters derived from the simulation of Ru K-edge EXAFS spectra of **1** before and after photoirradiation

	Bond	N^a	σ^2 (Å^2)	ΔE (eV)^b	R (Å)^c
Before photoirradiation	Ru–C(Cp)	4.2	0.002	18	2.310
	Ru–C(C_6H_6)	6.9	0.003	–7	2.158
After photoirradiation	Ru–C(Cp)	4.5	0.003	15	2.154
	Ru–N	3.7	0.004	–7	2.100

[a]Coordination number. [b]Energy shift. [c]Bond length.

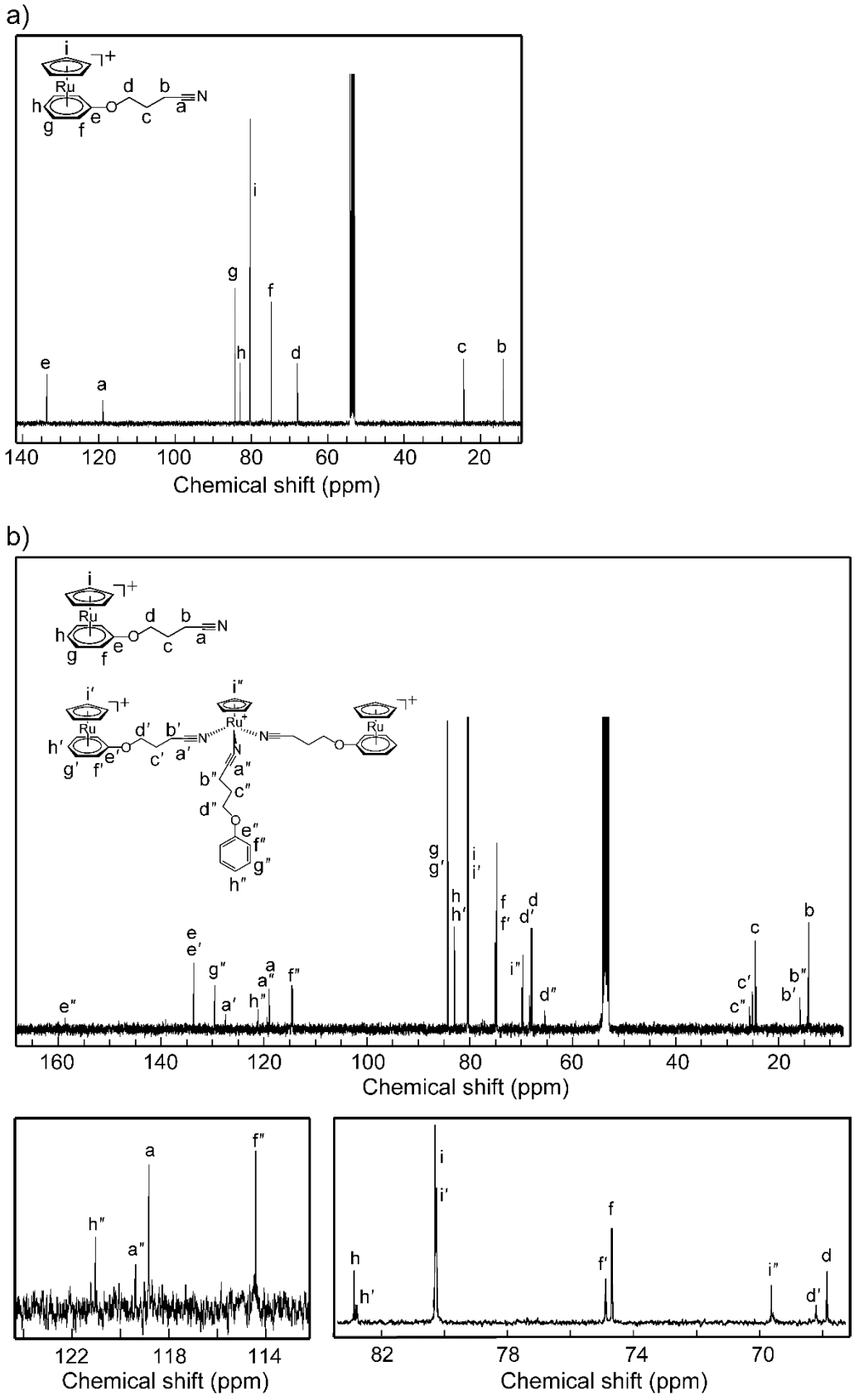

Fig. S2 ^{13}C NMR spectra of (a) **2** and (b) its photoproduct in CD_2Cl_2. The photoproduct contains unreacted **2**.

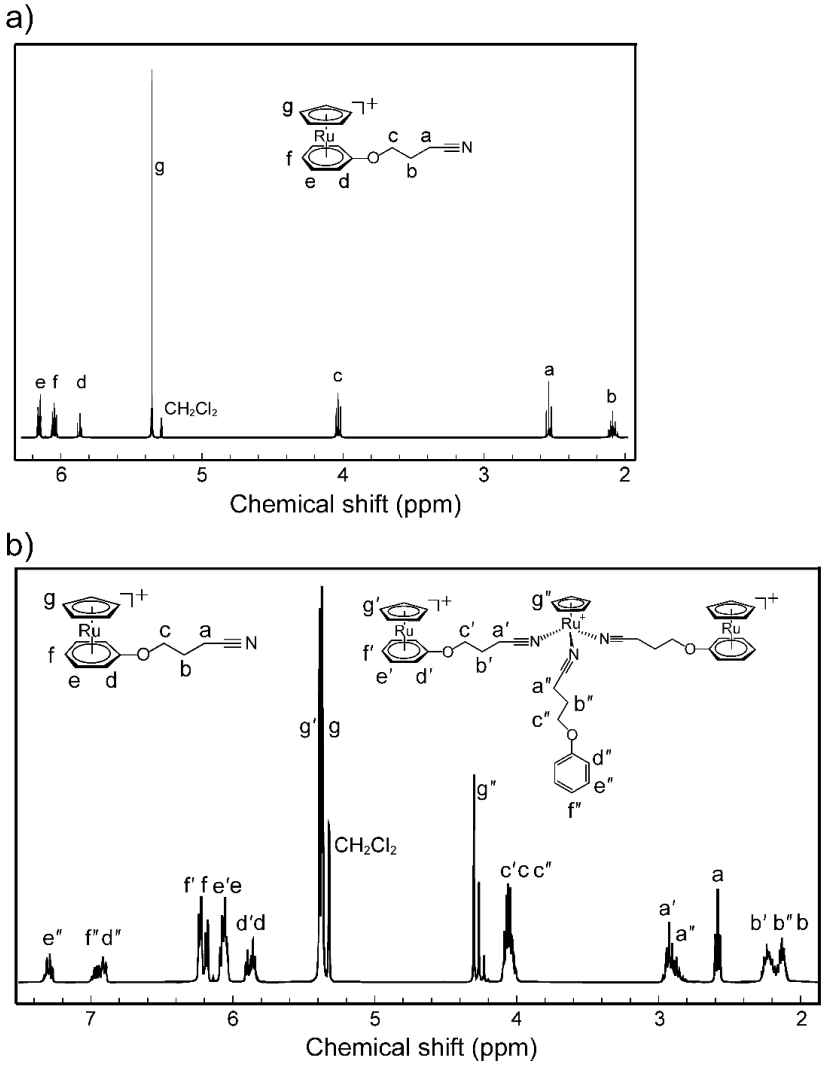

Fig. S3 ^{1}H NMR spectra of (a) **2** and (b) its photoproduct in CD_2Cl_2. The photoproduct contains unreacted **2**.

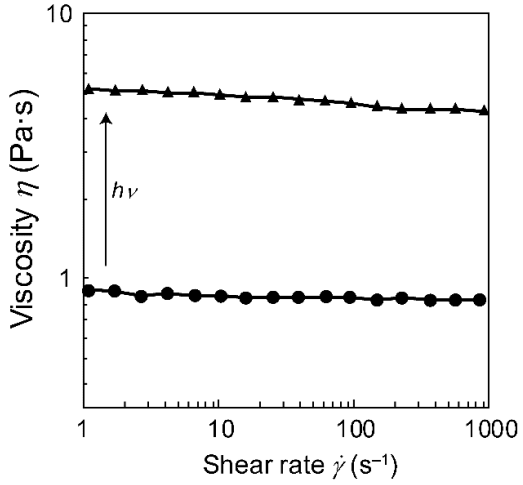

Fig. S4 Viscosity of ionic liquid **2** before and after photoirradiation (8 h) measured at 25 °C.